



OPEN

Pathogenesis of *CDK8*-associated disorder: two patients with novel *CDK8* variants and in vitro and in vivo functional analyses of the variants

Tomoko Uehara¹, Kota Abe^{2,6}, Masayuki Oginuma^{2,6}, Shizuka Ishitani^{2,6}, Hiroshi Yoshihashi³, Nobuhiko Okamoto⁴, Toshiki Takenouchi⁵, Kenjiro Kosaki¹ & Tohru Ishitani^{2,6}✉

Cyclin-dependent kinase 8 (CDK8) is a member of the CDK/Cyclin module of the mediator complex. A recent study reported that heterozygous missense *CDK8* mutations cause a neurodevelopmental disorder in humans. The mechanistic basis of *CDK8*-related disorder has yet to be delineated. Here, we report 2 patients with de novo missense mutations within the kinase domain of *CDK8* along with the results of in vitro and in vivo functional analyses using a zebrafish model. Patient 1 and Patient 2 had intellectual disabilities and congenital anomalies. Exome analyses showed that patient 1 had a heterozygous de novo missense p.G28A variant in the *CDK8* (NM_001260.3) gene and patient 2 had a heterozygous de novo missense p.N156S variant in the *CDK8* gene. We assessed the pathogenicity of these two variants using cultured-cells and zebrafish model. An in vitro kinase assay of human *CDK8* showed that enzymes with a p.G28A or p.N156S substitution showed decreased kinase activity. An in vivo assays of zebrafish overexpression analyses also showed that the p.G28A and p.N156S alleles were hypomorphic alleles. Importantly, the inhibition of *CDK8* kinase activity in zebrafish embryos using a specific chemical inhibitor induced craniofacial and heart defects similar to the patients' phenotype. Taken together, zebrafish studies showed that non-synonymous variants in the kinase domain of *CDK8* act as hypomorphic alleles causing human congenital disorder.

Cyclin-dependent kinase 8 (CDK8) is an evolutionarily conserved serine/threonine kinase that belongs to the CDK/Cyclin module of the mediator complex. *CDK8* modulates a variety of transcription regulators, including HIF1A, p53, and NRSF, both positively and negatively^{1–3} and controls signaling pathways, including the WNT/ β -catenin signaling pathway⁴.

A recent study reported the cases of 12 patients with eight heterozygous non-synonymous variants in the kinase domain (21–335 amino acids, Fig. 1a)⁵ of the *CDK8* gene who presented with characteristic facial features, congenital heart disorders and intellectual disability⁶. An in vitro functional analysis of the eight types of variants in the kinase domain of *CDK8* demonstrated that *CDK8*-associated disorder is caused by hypomorphic alleles of *CDK8*⁶. However, the mechanistic basis of *CDK8*-associated disorder in vivo has yet to be determined. In this article, we report an in vivo functional analysis in a zebrafish model with de novo amino-acid substitutions (p.G28A and N156S) in the kinase domain of *CDK8*, as detected in 2 patients with syndromic intellectual disability.

¹Center for Medical Genetics, Keio University Hospital, Tokyo, Japan. ²Institute for Molecular and Cellular Regulation, Gunma University, Maebashi, Japan. ³Department of Genetics, Tokyo Metropolitan Children's Medical Center, Tokyo, Japan. ⁴Department of Medical Genetics, Osaka Women's and Children's Hospital, Osaka, Japan. ⁵Department of Pediatrics, Keio University School of Medicine, Tokyo, Japan. ⁶Department of Homeostatic Regulation, Research Institute for Microbial Diseases, Osaka University, 3-1 Yamadaoka, Suita, Osaka 565-0871, Japan. ✉email: ishitani@biken.osaka-u.ac.jp

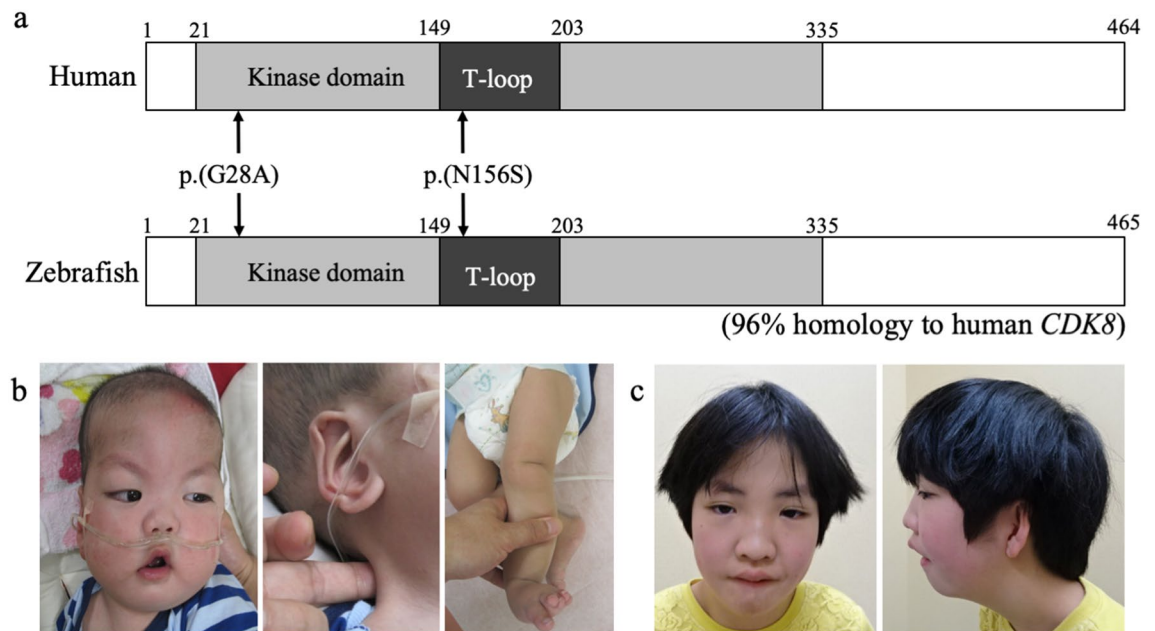


Figure 1. Schema of the CDK8 protein and clinical characteristics of our two patients with CDK8-associated disorder. **(a)** Schema of human CDK8 protein (the upper schema) and zebrafish Cdk8 protein (the lower schema). The grey box indicates the kinase domain. The black boxes indicate the T-loop in the kinase domain. The arrows point to the mutations of the 2 reported patients. **(b)** Patient 1 at 8 months of age. **(c)** Patient 2 at 8 years of age. In 1b, note the prominent forehead with large anterior fontanelle, arched eyebrow, hypertelorism, epicanthal folds, low-set ears, prominent antihelix, short philtrum, flat nasal bridge, high arched palate, downturned corners of the mouth, micrognathia, webbed neck, and overlapping toes on the left foot. In 1c, note the hypertelorism, epicanthal folds, wide nasal bridge, protruding ears, bifid uvula, and micrognathia.

Results

Clinical features. Patient 1 was a 3-year-old Japanese boy with a birth weight of 2246 g (-0.4 SD), a body length 46.5 cm ($+0.1$ SD), and a head circumference of 34 cm ($+1.3$ SD) who had been diagnosed at birth with a double outlet right ventricle, mitral valve stenosis, and dysmorphic craniofacial features. A Glenn operation was performed at 7 months of age. The patient had difficulty feeding and failed to thrive. Severe gastroesophageal reflux disease was treated by fundoplication and a gastrostomy. He also had an undescended left testis and left multicystic dysplastic kidney. A brain magnetic resonance imaging study showed agenesis of the corpus callosum. Markedly delayed motor development and language development had been observed since infancy. Generalized hypotonia was noted, and an eye examination revealed myopia.

On physical examination, his body height was 87.3 cm (-2.1 SD), his body weight was 10.9 kg (-1.9 SD), and his head circumference was 49.7 cm ($+0.1$ SD). Craniofacial dysmorphic features were observed and are described in Table 1 (Fig. 1b, Table 1); overlapping toes were noted on the left foot (Fig. 1b). Routine laboratory investigations and a metabolic survey yielded results within the normal range. A chromosomal analysis showed a normal male karyotype (46, XY), and array-based comparative genomic hybridization yielded normal results.

Patient 2 was an 8-year-old Japanese girl who had been diagnosed with pharyngostenosis and gastroesophageal reflux disease at 6 months of age. Her developmental milestones were delayed. At 8 years, 3 months, her body height was 115.8 cm (-2 SD), her body weight was 18.3 kg (-2.5 SD), and her head circumference was 52.0 cm (mean). She exhibited the dysmorphic features described in Table 1 (Fig. 1c, Table 1) as well as intermittent esotropia and pes planovalgus. At 8 years of age, her developmental quotient as assessed using the WISC-IV test was 52. She also exhibited tantrums, hyperactivity, agitation, emotional incontinence, and attention deficit.

Next-generation sequencing. An exome analysis of genomic DNA derived from peripheral blood samples from Patient 1 and Patient 2 showed a constitutional heterozygous de novo non-synonymous variant in exon 1 of the *CDK8* gene (NM_001260.3): c.83G>C, (p.Gly28Ala) and in exon 5 of the *CDK8* gene: c.467A>G, (p.Asn156Ser). We confirmed these findings using Sanger sequencing. The combined annotation-dependent depletion (CADD) scores⁷ for p.Gly28Ala and p.Asn156Ser were 23.9 and 26.2, respectively. The amino acid substitutions in CDK8 detected in these 2 patients were within the ATP-binding domain of the kinase domain of CDK8 protein (Fig. 1a)⁵. Neither of these variants was found in the normal 2048 Japanese database⁸ or in the ExAC database⁹.

In vitro kinase assay of human CDK8 containing G28A and N156S substitutions. First, to evaluate the functional relevance of the p.G28A and p.N156S amino acid substitutions in human CDK8 in vitro, we performed a kinase assay using HEK293 cells, which are suitable for the analysis of exogenous protein expres-

	Patient 1	Patient 2	Calpena et al. ⁶	14 patients with CDK8 variants
Variants in CDK8	c.83G > C (p.Gly28Ala)	c.467A > G (p.Asn156Ser)	c.79G > C (p.Val27Leu) c.85C > G (p.Arg29gly) c.88G > A (p.Gly30Ser) c.185C > T (p.Ser62Leu) × 5 c.291T > G (p.Phe97Leu) c.533G > A (p.Arg178Gln) c.578T > G (p.Val193Gly) c.669A > G (p.Ile223Met)	All 14 mutations were missense
Sex	Male	Female	7 males and 5 females	Male: 8, Female: 6
Developmental delay	Severe	Moderate	9/12	11/14
Intellectual disability	Severe	Moderate (WISC-IV IQ = 52)	11/12	13/14
Short stature	Present	Present	1/12	3/14
Hypotonia	Present	Present	9/11	11/13 (1 was not available)
Head and necks	Agenesis of corpus callosum	No abnormalities	Abnormality of corpus callosum: 4/9 (among 9 available patients)	Abnormality of corpus callosum: 5/11 (3 were not available)
Congenital heart disorders	DORV, mitral valve stenosis	Absent	Present: 6/10	7/12 (2 were not available)
Facial dysmorphology	Prominent forehead with large anterior fontanelle, arched eyebrow, hypertelorism, epicanthal folds, low set ears, prominent antihelix, a short philtrum, broad nasal root, a flat nasal bridge, a high arched palate, down turned corners of mouth, micrognathia	Arched eyebrow, ptosis, hypertelorism, epicanthal folds, broad nasal root, anteverted nares, a wide nasal bridge, protruding ears, bifid uvula, micrognathia	Arched eyebrow (3/12), epicanthal folds (4/12), ptosis (5/12), anteverted nares (3/12), broad nasal root (3/12), micrognathia (4/12)	Arched eyebrow (5/14), ptosis (5/14), epicanthal folds (6/14), broad nasal root (5/14), anteverted nares (5/14), micrognathia (6/14)
Behavioral/psychiatric manifestations	Absent	Tantrum, agitation, emotional incontinence, attention deficit-hyperactivity disorder (ADHD)	ADHD: 4/10, autism spectrum disorder: 5/10	ADHD: 5/12 (2 were not available)
Eye/vision	Myopia	Intermittent esotropia	Myopia: 5/12	Myopia (6/14)
Gastrointestinal problems	Gastroesophageal reflux disorder (GERD)	Absent	GERD: 3/12	GERD (4/14)
Urogenital problems	Left multicystic dysplastic kidney	Absent	0/12	1/14
Limbs	Absent	Pes planovalgus	Pes planovalgus: 2/12	3/14

Table 1. Summary of the patients with neurodevelopmental disorder and heterozygous variants in *CDK8*.

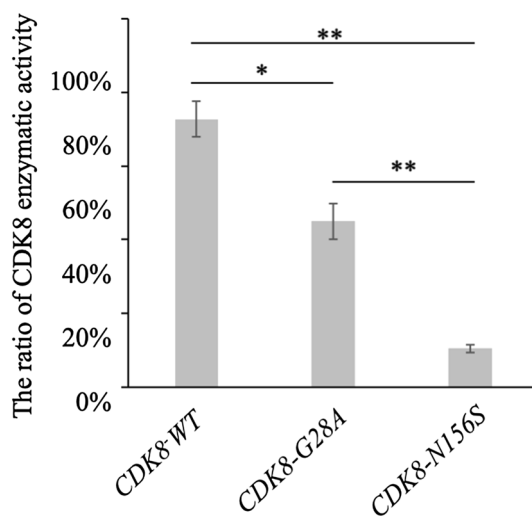


Figure 2. Results of human *CDK8* kinase assay. The graph shows the enzymatic activity rates of wild-type *CDK8*, G28A-mutated *CDK8*, and N156S-mutated *CDK8*. The error bars indicate the standard error of the mean (SEM). * $p < 0.05$, ** $p < 0.005$ using a t-test.

sion. Both the *CDK8-G28A* and *CDK8-N156S* mutations resulted in lower kinase activities compared with *CDK8-WT* (Fig. 2), and the kinase activity of *CDK8-N156S* was lower than that of *CDK8-G28A* (Fig. 2). These results also indicated that the 2 types of mutated *CDK8* were hypomorphic alleles.

In vivo functional assay of human *CDK8* containing G28A and N156S substitutions. Next, to evaluate the pathogenicity of the p.G28A and p.N156S amino-acid substitutions detected in Patient 1 and Patient

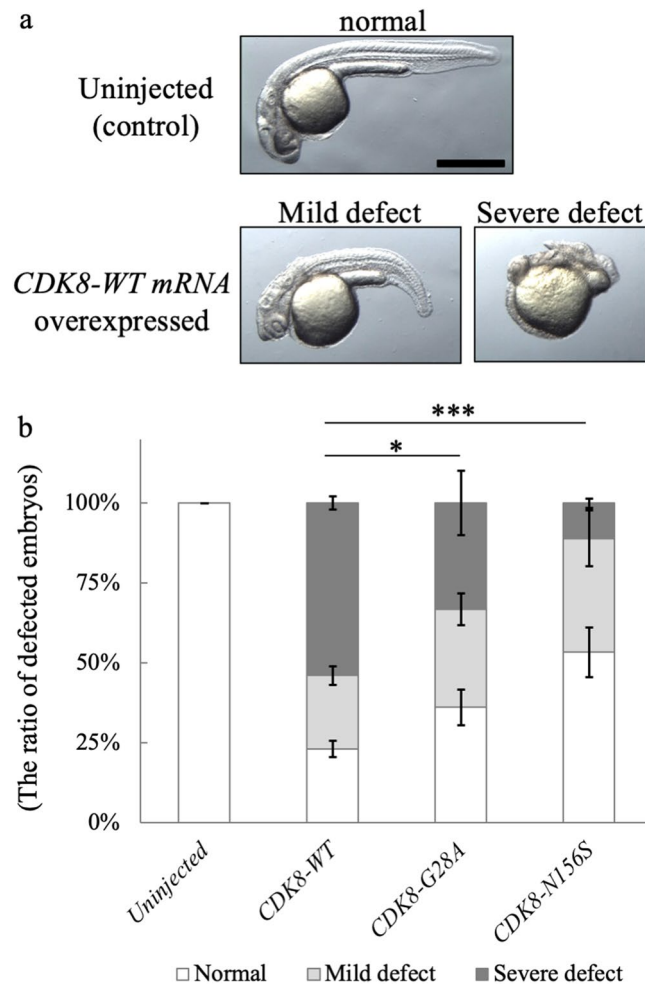


Figure 3. Results of *CDK8* mRNA overexpression analyses. **(a)** Photographs of zebrafish embryos at the 1-day post-fertilization (dpf) stage. An uninjected embryo was used as a control. The wild-type *CDK8* mRNA-injected embryo exhibited severe defects. Note that the *CDK8* mRNA injection induced a shortened body axis, small anterior structures, and an aberrant tail morphology. Scale bar, 500 μm . **(b)** Graph showing the proportions of abnormal zebrafish embryos. The error bars represent the SD for three independent experiments (for uninjected: $n = 15, 36, 63$ for *CDK8*: $n = 34, 35, 31$ for *CDK8-G28A*: $n = 26, 65, 63$ for *CDK8-N156S*: $n = 27, 23, 28$), $*p = 0.02117$, $***p = 6.224e-13$ using a chi-square test.

2, we injected zebrafish embryos with wild-type human *CDK8* mRNA (*CDK8-WT* mRNA) and 2 types of mutated human *CDK8* mRNA (i.e., *CDK8-G28A* mRNA and *CDK8-N156S* mRNA) and compared the zebrafish phenotypes at the 1-day post-fertilization (dpf) stage. Fraction of the embryos injected with *CDK8-WT* mRNA, *CDK8-G28A* mRNA, or *CDK8-N156S* mRNA exhibited a short body axis, hypoplastic anterior structures, and an aberrant tail (Fig. 3a).

The relative fraction of embryos with defects was largest when mRNA encoding the human wild-type *CDK8* protein was injected (Fig. 3b). This observation indicated that *CDK8-G28A* and *CDK8-N156S* are hypomorphic alleles. In addition, consistent with the results of the in vitro kinase assays, the defect-inducing activity of *CDK8-N156S* was lower than that of *CDK8-G28A* (Fig. 3b), suggesting that the N156A mutation severely reduces *CDK8* activity, while the G28A mutation mildly reduces the activity.

Chemical inhibition of *Cdk8* in zebrafish. We investigated whether the addition of Senexin A which inhibits *CDK8* and its paralogous *CDK19* would induce phenotypes reminiscent of the patients, and the results showed that the inhibition of *Cdk8* kinase activity by Senexin A induced structural anomalies in the heart and craniofacial cartilage of the zebrafish (Fig. 4c,d, $n = 46, 100\%$) compared to the control embryo (Fig. 4a,b) and disturbed blood circulation (Supplementary Video S1 and S2).

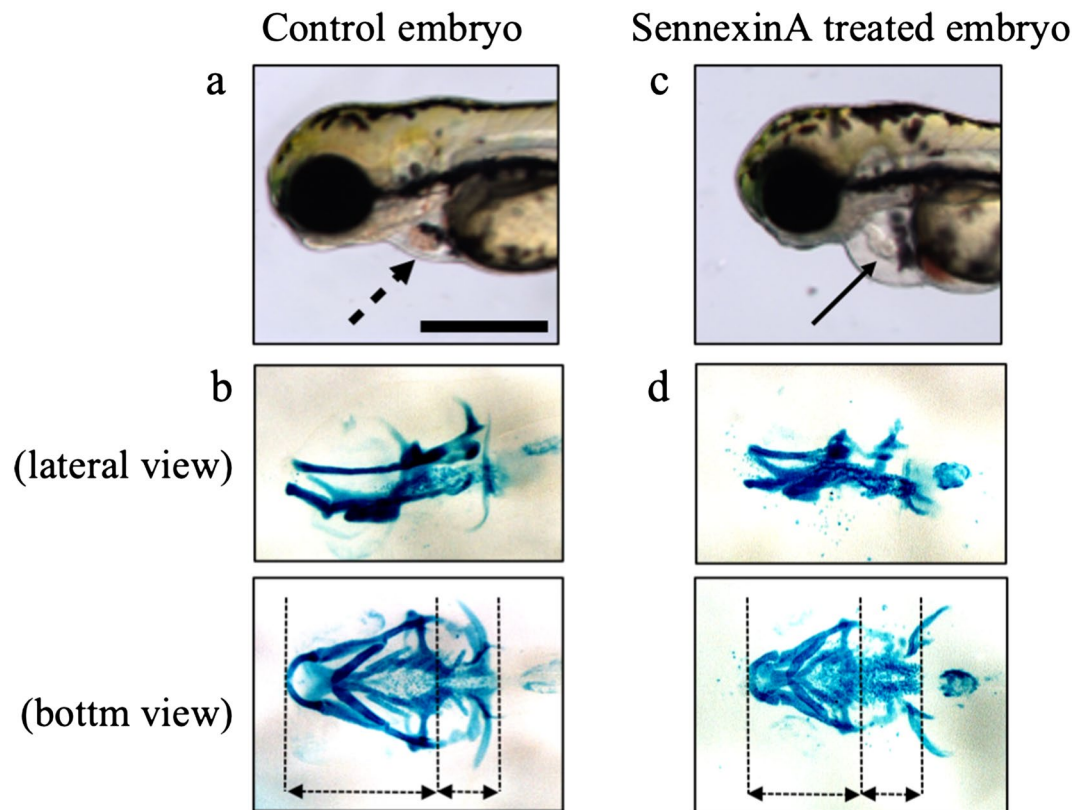


Figure 4. Results of chemical inhibition of Cdk8 in zebrafish. Photographs of the cranial cartilage of zebrafish embryos exposed to Senexin A at the 5 dpf stage. The upper photographs (a,c) are lateral view, and the lower photographs (b,d) are ventral view of the same embryo. (a,b) are photographs of a control embryo, and (c,d) are photographs of a Senexin A-exposed embryo. Note the cranial anomaly and shortened head in the fish. Scale bar in a, 0.2 mm.

Discussion

We showed herein that *CDK8*-associated disorder is caused by a reduction in CDK8 function using an in vivo functional assay, as supported by a previously reported in vitro assay⁶. We presented the cases of two patients with *CDK8*-associated disorder and suggested that craniofacial and cardiac defects are critical components of the newly identified disorder.

In this study, an in vivo functional study in a zebrafish model showed that the G28A and N156S mutations in the *CDK8* gene detected in the two presently reported patients were hypomorphic alleles (Fig. 3). We also showed that the in vitro kinase activities of CDK8-G28A and CDK8-N156S proteins, which were produced in human embryonic kidney (HEK293) cells, were significantly lower than that of the wild-type CDK8 protein (Fig. 2). These results agree with the observation of kidney defects in a patient with a *CDK8* mutation. In addition, the results of our in vivo and in vitro assays were consistent with those of a previous study⁶.

The reduction of the CDK8 activity induced by N156S mutation was larger than that induced by G28A mutation. Furthermore, relative fraction of embryos with severe defects was larger after injection of mRNA encoding the G28A mutant proteins than after injection of mRNA encoding the N156S. Hence, both the in vitro kinase assays and the zebrafish in vivo assays showed that the N156S variant had a stronger effect than the G28A variant. This in vitro and in vivo results may be due to that N156 is more critical for CDK8 kinase activity, comparing with G28. Consistent with this idea, N156 is a highly conserved residue between CDK family kinases and locates on the T-loop, which is required for Cdk activation, while G28 is conserved between only a part of CDKs.

In humans and zebrafish, CDK8 has a paralog called CDK19 (also known as CDK8L), and CDK8 and CDK8L/CDK19 are generally assumed to have redundant roles. The current observation that the two patients with *CDK8* mutations were symptomatic even in the presence of intact CDK19 suggests that CDK8 and CDK19 are not completely redundant from a functional standpoint. Furthermore, since mutant kinases lacking catalytic activity often confer a dominant-negative effect through interactions with their endogenous substrate and regulators, the mutant CDK8 protein might have interfered with the normal CDK19 protein.

Our observation that Senexin A, which inhibits CDK8, induced phenotypes reminiscent of those in the patients with *CDK8* mutations supports the notion that *CDK8* mutations confer a hypomorphic effect. This observation, however, needs to be interpreted with caution, since Senexin A inhibits both CDK19 and CDK8. At the same time, one could argue that the inhibitory action of Senexin A on both CDK19 and CDK8 may indeed mimic the presumable dominant-negative effect of the *CDK8* mutations on CDK19 as well. Overall, the results

of our *in vivo* analyses provide further credence to the notion that *CDK8*-associated disorder is caused by a functional reduction of *CDK8*, as suggested by the *in vitro* assay reported by Calpena et al.⁶

In this study, we further defined the characteristic phenotypes of the newly identified disorder described in the initial report⁶. The characteristic features of our two patients and the 12 patients in the initial report⁶ are summarized in Table 1. Thirteen of the 14 patients had neurodevelopmental disabilities, and Patients 1 and 6 of the previously reported patients had congenital heart disorders. Common characteristic facial features include arched eyebrows (5/14), epicanthal folds (4/14), ptosis (6/14), anteverted nares (5/14), broad nasal root (5/14), and micrognathia (6/14). The neurodevelopmental abnormalities, congenital heart disorders, and facial features described above are characteristics of *CDK8*-associated developmental disorder. The phenotypes seem diverse, but the phenotypes of the *Cdk8*-knockdown zebrafish in the *in vivo* functional assay in our study were comparable to the phenotypes of patients with *CDK8*-associated disorder.

In conclusion, the results of this study suggest that *CDK8*-associated disorder is caused by the functional loss of *CDK8* kinase activity. The phenotypes of the newly identified disorder are intellectual disability, characteristic facial features, and multiple organ defects. The phenotypes exhibited in the zebrafish model described above were comparable to the patients' phenotypes.

Methods

Genetic analysis. Approval from the local institutional review board and informed consent from the patients' parents were obtained prior to the molecular studies. DNA from peripheral blood samples obtained from the patients and their parents were isolated and subjected to exome sequencing with a SureSelect XT Human All Exon V6 Panel (Agilent Technology, Santa Clara, CA) on a HiSeq platform (Illumina, San Diego, CA). We confirmed the results by performing Sanger sequencing with the following primers: *CDK8_Patient 1_sense*, 5'-GCT CTT GCC GCA TCA GTC-3'; *CDK8_Patient 1_antisense*, 5'-GGC GTC GAG GAA GTC AGA G-3'; *CDK8_Patient 2_sense*, 5'-CAT GCA CAG TTT CTT TGG TGA C-3'; and *CDK8_Patient 2_antisense*, 5'-TGG CTT CGA TCA TAT GGA ACT AC-3'.

***In vivo* functional assay.** We performed *in vivo* functional analyses using a zebrafish model because zebrafish have a homologue of human *CDK8*, *Cdk8*. *Cdk8* shares 96% homology with human *CDK8* (Fig. 1a), and the sequences around the two reported variants are conserved in *Cdk8*. To determine whether the two variants reported in our patients were hypomorphic alleles, we compared the phenotypes of zebrafish injected with human *CDK8-WT* mRNA with those of zebrafish injected with mutated *CDK8* mRNA by performing the following experiment. First, we cloned the cDNA of wild-type human *CDK8* (a gift from Dr. Conaway, Addgene #15366)¹⁰ into the pCS2p+ Flag vector in-frame of the Flag tag. The Gly28Ala (*CDK8-G28A*) and Asn152Ser (*CDK8-N156S*) point mutations identified in the patients' DNA were then introduced into human *CDK8* gene using a QuikChange Site-Directed Mutagenesis kit (Agilent). Next, capped mRNA was synthesized using a SP6 mMESSAGE mMACHINE kit (Ambion, Austin, TX). The cDNA of wild-type human *CDK8* (a gift from Dr. Conaway, Addgene #15366)¹⁰ capped mRNA was synthesized using an SP6 mMESSAGE mMACHINE kit (Ambion, Austin, TX) and purified on Micro Bio-Spin columns (Bio-Rad, Hercules, CA). We injected each of the synthesized mRNAs (*CDK8-WT*: n = 34, 35, 31, *CDK8-G28A*: n = 26, 65, 63, and *CDK8-N156S*: n = 27, 23, 28) into one-cell stage embryos (150 pg) and examined the morphological features at the 1-day-post-fertilization (dpf) stage of the embryos. The proportion of the phenotypes was determined by pooling the data from all three replicates and conducting a Chi-square test for *CDK8-G28A* or *CDK8-N156S* against *CDK8-WT*.

Kinase assay. Flag-*CDK8* and its mutants were expressed with CyclinC in HEK293 cells and immunoprecipitated with anti-Flag antibody. Immunoprecipitates were purified by washing six times with PBS. Aliquots of immunoprecipitated *CDK8* proteins were incubated for 90 min with or without 50 μ M ATP in 40 μ L of kinase buffer containing 40 mM Tris (pH7.5), 100 μ M BSA, and 20 mM MgCl₂ at 25 °C, and the ADP produced by *CDK8* autophosphorylation was measured using an ADP-GLO Kinase Assay kit (Promega). Immunoprecipitates from cells transfected with empty vector was used for measurement of background activity. The values shown are the average of the values observed in one representative experiment in which each transfection was performed in triplicate.

Chemical inhibition of *Cdk8* activity by Senexin A. The phenotypes of *Cdk8* inhibition were investigated in zebrafish by treatment with the *Cdk8/Cdk19*-specific inhibitor Senexin A (2 μ M) from 18 dpf. We then compared the phenotypes of the Senexin A-exposed zebrafish and the control zebrafish.

Cartilage staining. To observe head formation, we performed cartilage staining using the following method. At 6 days post-fertilization, the embryos were fixed overnight in 4% paraformaldehyde/PBS. They were then dehydrated with ethanol and stained with 0.02% Alcian blue in an acid solution (40% acetic acid, 60% ethanol). After rehydration, the embryos were cleared in 2% KOH, bleached in 3% H₂O₂, and further cleared in glycerol.

Ethics statement. All studies in this paper were approved by the local Institutional Review Board in Keio University School of Medicine, Ethics Committee, Gunma University, and Osaka University. All human studies were performed in accordance with the ethical standards of the Declaration of Helsinki. All experimental animal care was performed in accordance with institutional and national guidelines and regulations. The study protocol

was approved by the Institutional Animal Care and Use Committee of the respective universities (Gunma University Permit# 17-051; Osaka University, RIMD Permit#R02-04-0).

Received: 13 October 2019; Accepted: 3 September 2020

Published online: 16 October 2020

References

1. Ding, N. *et al.* Mediator links epigenetic silencing of neuronal gene expression with X-linked mental retardation. *Mol. Cell* **31**, 347–359 (2008).
2. Donner, A. J., Szostek, S., Hoover, J. M. & Espinosa, J. M. CDK8 is a stimulus-specific positive coregulator of p53 target genes. *Mol. Cell* **27**, 121–133 (2007).
3. Galbraith, M. D. *et al.* HIF1A employs CDK8-mediator to stimulate RNAPII elongation in response to hypoxia. *Cell* **153**, 1327–1339 (2013).
4. Firestein, R. *et al.* CDK8 is a colorectal cancer oncogene that regulates beta-catenin activity. *Nature* **455**, 547–551 (2008).
5. Xu, W. & Ji, J. Y. Dysregulation of CDK8 and Cyclin C in tumorigenesis. *J. Genet. Genomics* **38**, 439–452 (2011).
6. Calpena, E. *et al.* De novo missense substitutions in the gene encoding CDK8, a regulator of the mediator complex, cause a syndromic developmental disorder. *Am. J. Hum. Genet.* **104**, 709–720 (2019).
7. Kircher, M. *et al.* A general framework for estimating the relative pathogenicity of human genetic variants. *Nat. Genet.* **46**, 310–315 (2014).
8. Nagasaki, M. *et al.* Rare variant discovery by deep whole-genome sequencing of 1,070 Japanese individuals. *Nat. Commun.* **6**, 8018 (2015).
9. Lek, M. *et al.* Analysis of protein-coding genetic variation in 60,706 humans. *Nature* **536**, 285–291 (2016).
10. Conaway, R. C., Sato, S., Tomomori-Sato, C., Yao, T. & Conaway, J. W. The mammalian mediator complex and its role in transcriptional regulation. *Trends Biochem. Sci.* **30**, 250–255 (2005).

Acknowledgements

We thank Mrs. Chika Kanoe, Mrs. Yumi Obayashi, and Mrs. Keiko Tsukue for their technical assistance in the preparation of this article. Informed consents were obtained from each patient's parents for publishing patients pictures in Fig. 1.

Author contributions

U.T. and K.K. wrote the main manuscript text. K.A., M.O., S.I., and T.I. designed and performed all the experiments. U.T., H.Y., N.O., T.T., and K.K. have contributed to data collection and interpretation, and critically reviewed the manuscript. All authors contributed to analysis and interpretation of data. All authors agree to be accountable for all aspects of the work in ensuring that questions related to the accuracy or integrity of any part of the work are appropriately investigated and resolved.

Funding

This work was supported by the Japan Agency for Medical Research and Development under Grant Numbers JP18ek0109301, JP19ek0109301, JP18ek0109288h0002, JP19ek0109288h0003, and JP20ek0109484h0001, the Grant-in-Aid for Scientific Research (B) under Grant Number 19H03412, and the Grant-in-Aid for Scientific Research (C) under Grant Numbers 19K06673 and 20K07322.

Competing interests

The authors declare no competing interests.

Additional information

Supplementary information is available for this paper at <https://doi.org/10.1038/s41598-020-74642-4>.

Correspondence and requests for materials should be addressed to T.I.

Reprints and permissions information is available at www.nature.com/reprints.

Publisher's note Springer Nature remains neutral with regard to jurisdictional claims in published maps and institutional affiliations.



Open Access This article is licensed under a Creative Commons Attribution 4.0 International License, which permits use, sharing, adaptation, distribution and reproduction in any medium or format, as long as you give appropriate credit to the original author(s) and the source, provide a link to the Creative Commons licence, and indicate if changes were made. The images or other third party material in this article are included in the article's Creative Commons licence, unless indicated otherwise in a credit line to the material. If material is not included in the article's Creative Commons licence and your intended use is not permitted by statutory regulation or exceeds the permitted use, you will need to obtain permission directly from the copyright holder. To view a copy of this licence, visit <http://creativecommons.org/licenses/by/4.0/>.

© The Author(s) 2020